

# CALCULATION OF INELASTIC NOTCH-TIP STRAIN-STRESS HISTORIES UNDER CYCLIC LOADING

G. GLINKA<sup>†</sup>

Department of Mechanical Engineering, University College London, Torrington Place,  
London, WC1E 7JE England

**Abstract**—An application of the equivalent strain energy density method for calculation of elastic-plastic notch-tip strains under cyclic loading is presented. It is shown that the theoretical notch-tip strain calculations can be improved if the stress redistribution due to the plastic yielding around the notch-tip is taken into account. The energy density method, corrected for plastic yielding gave good results almost up to the general plastic yielding, i.e.  $S = \sigma_{ys}$ . It was also found that a universal function for the elastic stress distribution ahead of a notch tip can be derived for both tension and bending loads. Several different notches and materials were analyzed. The equivalent strain energy density concept can easily be used for a simulation of the notch-tip cyclic stress-strain history if the stress concentration factor  $K_t$ , the cyclic stress-strain curve  $\sigma - \epsilon$  and nominal stress/load history are known. Good notch-tip strain predictions were achieved for both the monotonic and cyclic load.

## NOTATION

- $C_p$  strain energy density correction factor for plastic yielding.  
 $E$  modulus of elasticity  
 $e_t$  nominal notch-tip strain  
FEM finite element method  
 $K$  stress intensity factor  
 $K_t$  stress concentration factor  
 $k$  strength coefficient  
 $k'$  cyclic strength coefficient  
 $L$  distance from the notch tip to the neutral axis in bending  
 $M$  bending moment  
 $n$  strain hardening exponent  
 $n'$  cyclic strain hardening exponent  
 $P$  load (force)  
 $r$  radial polar coordinate  
 $r_p$  the first approximation of the plastic zone size  
 $\Delta r_p$  increment of the plastic zone due to the stress redistribution caused by plastic yielding  
 $S$  nominal stress  
 $S_t$  nominal notch-tip stress  
 $\Delta S_t$  nominal stress range in the notch tip  
 $W_c$  notch-tip strain energy density corrected for plastic yielding  
 $W_e$  notch-tip strain energy density due to the elastic stress  $\sigma_{te}$   
 $W_p$  notch-tip strain energy density due to the elastic-plastic stress  $\sigma_{tp}$   
 $W_s$  notch-tip strain energy density due to the nominal stress  $S_t$   
 $x_0 = L/\rho$  nondimensional distance from the notch tip to the neutral axis in bending  
 $\epsilon$  strain  
 $\epsilon_{ee}$  elastic part of the total strain  
 $\epsilon_{pp}$  plastic part of the total strain  
 $\epsilon_{te}$  elastic strain at the notch tip  
 $\epsilon_{tp}$  elastic-plastic strain at the notch tip  
 $\epsilon_{tp}^p$  elastic-plastic strain at the notch tip in plane strain  
 $\epsilon_{tp}^{\max}$  maximum elastic-plastic strain at the notch tip  
 $\epsilon_{tp}^{\min}$  minimum elastic-plastic strain at the notch tip  
 $\epsilon_N$  notch tip strain calculated from Neuber's rule  
 $\Delta\epsilon_{tp}$  elastic-plastic notch-tip strain range  
 $\mu$  generalized Poisson coefficient  
 $v$  Poisson's coefficient  
 $\rho$  notch-tip radius  
 $\sigma$  stress  
 $\sigma_x, \sigma_y, \sigma_z$  elastic stress components  
 $\sigma_{yp}$  elastic-plastic stress component  $\sigma_y$  ahead of the crack tip  
 $\sigma_y(r_p)$  stress  $\sigma_y$  at the elastic-plastic boundary  
 $\sigma_{ys}$  yield strength

<sup>†</sup>On leave from Warsaw Technical University, Warsaw, Poland.

$\sigma_{te}$	elastic stress at the notch tip
$\sigma_{tp}$	elastic-plastic stress at the notch tip
$\sigma_{tp}^p$	elastic-plastic stress at the notch tip in plane strain
$\sigma_{tp \max}$	maximum elastic-plastic stress at the notch tip
$\sigma_{tp \min}$	minimum elastic-plastic stress at the notch tip
$\sigma_N$	notch-tip stress calculated from Neuber's rule
$\Delta\sigma_{tp}$	elastic-plastic notch-tip stress range

## 1. INTRODUCTION

THE LOCAL inelastic stress and strains near notches are very important for fatigue life analysis of notched components[1]. However, accurate calculations of these strains are difficult and lengthy. Therefore several approximate methods[2] are presently used. The most frequently used is Neuber's[3] rule, which was generalized lately by Seeger and Heuler[4]. Topper *et al.* have extended Neuber's rule to cyclic loading situations[5], and its suitability in fatigue predictions was the subject of several studies[1, 6, 7]. However, it was found[6, 7, 8] that Neuber's rule often overestimates the notch-tip inelastic strains and stresses. In order to compensate for this effect, the lower value of the fatigue notch factor  $K_f$  was suggested instead of the theoretical stress concentration  $K_t$ . Such a substitution made it possible to improve the fatigue life prediction sometimes, but it did not improve the accuracy of the calculated notch strains. The elastic stress concentration at a notch tip depends on the geometry of the notched body, and it is the same for monotonic and cyclic loadings. The overestimation of the inelastic strains and stresses at the notch tip was not caused by the decrease of stress concentration due to a cyclic loading, which was indirectly assumed by using fatigue notch factor  $K_f$ , but it was probably due to the approximate nature of Neuber's rule. Therefore, the method based on equivalent strain energy density concept has been proposed[9]. It was shown[10] that the method made it possible to calculate the inelastic notch-tip strains under static loadings in several notches and materials. Application of the improved equivalent strain energy density method for notches under cyclic loading histories is presented below.

## 2. THE HYPOTHESIS OF EQUIVALENT STRAIN ENERGY DENSITY AT A NOTCH TIP

It has been shown by Hutchinson[11] that, in the case of a material characterized by the bilinear stress-strain behaviour, the strain energy density distribution in the plastic zone ahead of a crack tip was the same as that calculated on the basis of the linear elastic stress-strain analysis. Molski and Glinka[9] have assumed that it was also true for notches and materials exhibiting nonlinear stress-strain behaviour. It means that in the presence of localised plastic yielding ahead of a notch tip the energy density at the notch tip can be calculated on the basis of the theoretical elastic stress distribution. Subsequently the energy density can be translated into the elastic-plastic strains and stresses which actually exist at the notch tip (Fig. 1). It is also necessary to know the nonlinear stress-strain curve of the analyzed material.

In the case of the elastic material behaviour the local stresses at the notch tip can be calculated as

$$\begin{cases} \sigma_y = \sigma_{te} = S_t K_t, \\ \sigma_x = \sigma_z = 0 \end{cases} \quad \text{for plane stress,} \quad (1)$$

and

$$\begin{cases} \sigma_y = \sigma_{te} = S_t K_t, \\ \sigma_x = 0, \\ \sigma_z = \nu \sigma_{te} \end{cases} \quad \text{for plane strain.} \quad (2)$$

It is apparent that in the plane stress conditions a uniaxial stress state exists at the notch tip, and therefore uniaxial stress-strain relations can be used.

$$\epsilon_{te} = \sigma_{te}/E \quad \text{for elastic behaviour,} \quad (3)$$

$$\epsilon_{tp} = \sigma_{tp}/E + (\sigma_{tp}/k)^{1/n} \quad \text{for elastic-plastic behaviour.} \quad (4)$$

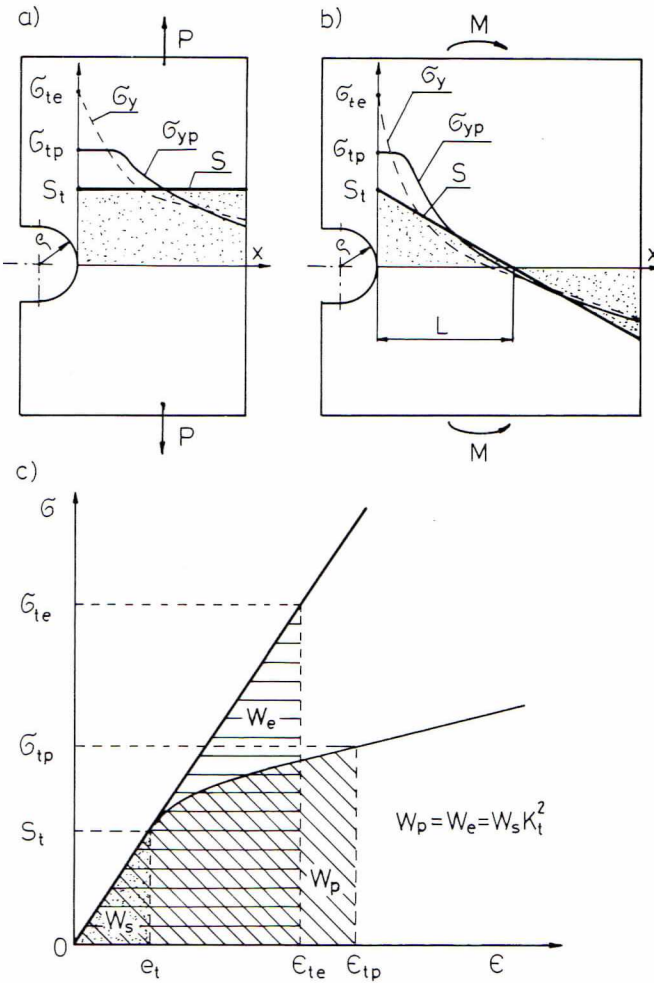


Fig. 1. Stress distribution in notched specimens and the strain energy density concept. (a) Notched specimen under tension loading. (b) Notched specimen under bending loading. (c) Graphical interpretation of the equivalent energy density concept.

Thus, the strain energy density at the notch tip[9] can be calculated as

$$W_e = \int_0^{\epsilon} \sigma \cdot d\epsilon = \frac{1}{2} \sigma_{te} \cdot \epsilon_{te} = \frac{\sigma_{te}^2}{2E}. \quad (5)$$

Substituting the stress  $\sigma_{te}$  by relation (1) we have

$$W_e = (S_t K_t)^2 / 2E. \quad (6)$$

Also, the energy density due to the nominal stress  $S_t$  can be written in the form of eqn (7):

$$W_s = S_t^2 / 2E. \quad (7)$$

Finally, the relation between the strain energy density at the notch tip and the strain energy density due to the nominal stress can be written

$$W_e = W_s \cdot K_t^2. \quad (8)$$

It was assumed that relation (8) is also valid when localized plastic yielding occurs ahead of the notch tip.

$$W_p = W_s K_t^2. \quad (9)$$

However, in the latest case the energy density at the notch tip must be calculated on the basis of the nonlinear stress-strain curve represented often by the Ramberg-Osgood relation (4).

$$W_p = \int_0^\epsilon \sigma \, d\epsilon = \frac{\sigma_{tp}^2}{2E} + \frac{\sigma_{tp}}{n+1} \left( \frac{\sigma_{tp}}{k} \right)^{1/n}. \quad (10)$$

Thus, eqn (9) can be written as

$$\frac{\sigma_{tp}^2}{2E} + \frac{\sigma_{tp}}{n+1} \left( \frac{\sigma_{tp}}{k} \right)^{1/n} = \frac{S_t^2}{2E} K_t^2. \quad (11)$$

It was also shown[10, 12] that the validity of eqn (9) could be extended if the stress-strain nonlinearity occurring under nominal stress  $S_t$  were taken into account. It means that the small nonlinearity just below the yield limit  $\sigma_{ys}$  should be included into calculations.

$$W_s = \frac{S_t^2}{2E} + \frac{S_t}{n+1} \left( \frac{S_t}{k} \right)^{1/n}. \quad (12)$$

This leads to further generalization of eqn (9).

$$\frac{\sigma_{tp}^2}{2E} + \frac{\sigma_{tp}}{n+1} \left( \frac{\sigma_{tp}}{k} \right)^{1/n} = \left[ \frac{S_t^2}{2E} + \frac{S_t}{n+1} \left( \frac{S_t}{k} \right)^{1/n} \right] \cdot K_t^2. \quad (13)$$

Finally, one has to solve a set of two equations for calculating the inelastic stress and strain at the notch tip.

$$W_p = W_s \cdot K_t^2, \quad \epsilon_{tp} = \frac{\sigma_{tp}}{E} + \left( \frac{\sigma_{tp}}{k} \right)^{1/n}. \quad (14)$$

It should be pointed out that, with the aid of a computer, any stress-strain relation can be handled, and the method does not need to be limited to the Ramberg-Osgood (4) relation only. It was shown[10] that the linear piecewise representation of the stress-strain curve can be used for numerical calculations.

An analogous analysis can be presented for the plane strain conditions, where again the stress component  $\sigma_y$  contributes only to the strain energy density at a notch tip. However, due to the biaxial stress state at the notch tip, the uniaxial stress-strain curve cannot be used. Therefore, Dowling *et al.*[13] suggested that the  $\sigma$ - $\epsilon$  relation, corrected for the biaxial stress state, should be used. By applying Hooke's law and von Mises's criterion for the elastic and plastic terms of the stress-strain relation (4), respectively, Dowling *et al.*[13] have derived the following relationships for the translation of the uniaxial stress-strain curve  $\sigma_{tp}$ - $\epsilon_{tp}$  into the biaxial "plane-strain" relation  $\sigma_{tp}^b$ - $\epsilon_{tp}^b$ .

$$\epsilon_{tp}^b = \epsilon_{tp}(1 - \mu^2)/\sqrt{(1 - \mu - \mu^2)}, \quad (15)$$

$$\sigma_{tp}^b = \sigma_{tp}/\sqrt{(1 - \mu - \mu^2)}, \quad (16)$$

where

$$\mu = \frac{\nu + E\epsilon_{pp}/2\sigma_{tp}}{1 + E\epsilon_{pp}/\sigma_{tp}}, \quad \epsilon_{tp} = \frac{\sigma_{tp}}{E} + \epsilon_{pp} = \epsilon_{ee} + \epsilon_{pp}.$$

Thus, under plane strain conditions the same set of equations (14) can be used, except that all calculations must be based on the "plane-strain" stress-strain curve  $\sigma_{tp}^b$ - $\epsilon_{tp}^b$ .

However, it was found[10] that under a high nominal stress  $S_t$  and a high stress concentration factor  $K_t$ , the energy-based method underestimated slightly the notch-tip inelastic

stresses and strains. This occurred because of the local stress redistribution caused by the plastic yielding around the notch tip.

#### Plastic zone adjustment

Because of plastic yielding the real stresses in the plastic zone are lower than those derived on the basis of the linear-elastic analysis. In order to satisfy the equilibrium conditions of the notched body, a stress redistribution occurs in the neighbourhood of the notch tip, (Fig. 2) resulting in an increase of the plastic zone size. Such increases of the plastic zone size can be interpreted analogously with Irwin[14], as an increase of the hypothetical elastic stresses. In the case of sharp notches or cracks such an increase of the plastic zone size causes a proportional increment of the energy density ahead of the notch tip.

$$W_c = W_e \left( \frac{r_p + \Delta r_p}{r_p} \right) = W_s K_t^2 \left( 1 + \frac{\Delta r_p}{r_p} \right). \quad (17)$$

Substituting the right side of equation (14) by the relation (17) a new set of two equations, necessary for calculating the notch-tip strains and stresses, can be derived.

$$W_c = W_s K_t^2 C_p, \quad (18)$$

$$\epsilon_{tp} = \sigma_{tp}/E + (\sigma_{tp}/k)^{1/n}, \quad (19)$$

where

$$C_p = 1 + \Delta r_p/r_p \quad (18a)$$

Solving the above set of equations requires an estimation of the plastic zone size ahead of the notch. Therefore the elastic stress field ahead of the notch tip must also be determined.

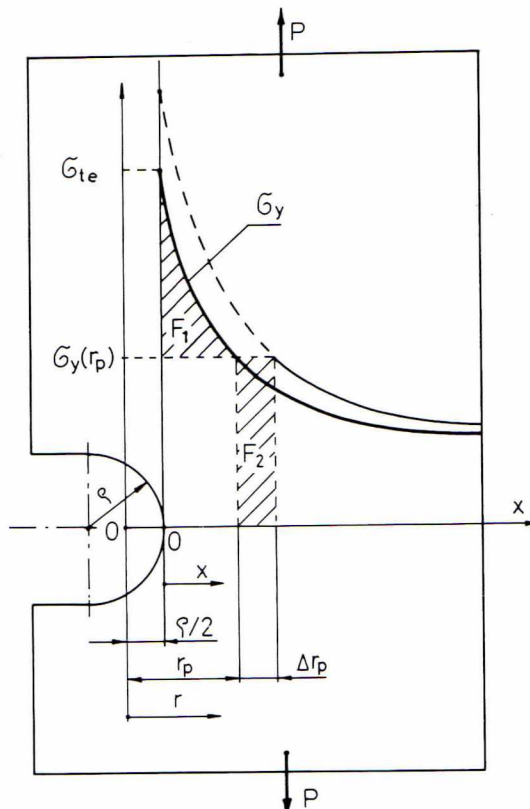


Fig. 2. Plastic yielding and the elastic stress redistribution ahead of a notch tip.

*Universality of the stress field in the vicinity of a notch tip*

It was shown by Creager and Paris[15] that the stress field in the close neighbourhood of the notch tip can be given in general form in terms of stress intensity factor  $K$ .

$$\sigma_x = \frac{K}{(2\pi r)} \left( 1 - \frac{\rho}{2r} \right), \quad (20)$$

$$\sigma_y = \frac{K}{(2\pi r)} \left( 1 + \frac{\rho}{2r} \right), \quad (21)$$

$$\sigma_z = 0 \quad \text{for plane stress,}$$

$$\sigma_z = \nu(\sigma_x + \sigma_y) \quad \text{for plane strain.}$$

It should be noted that the origin of polar coordinates used by Creager and Paris is at a distance of  $\rho/2$  behind the notch tip.

For  $r = \rho/2$  the stress at the notch tip  $\sigma_{te}$  and the stress concentration  $K_t$  can be calculated.

$$\sigma_{te} = 2K/\sqrt{(\pi\rho)}, \quad (22)$$

$$K_t = \sigma_{te}/S_t = 2K/S_t\sqrt{(\pi\rho)}; \quad (23)$$

hence,

$$K = K_t S_t \sqrt{(\pi\rho)}/2. \quad (24)$$

Substituting relation (24) for the stress intensity factor  $K$  in equations (20) and (21), we get

$$\sigma_x = \frac{K_t S_t}{2\sqrt{2}} \left[ \left( \frac{\rho}{r} \right)^{1/2} - \frac{1}{2} \left( \frac{\rho}{r} \right)^{3/2} \right], \quad (25)$$

$$\sigma_y = \frac{K_t S_t}{2\sqrt{2}} \left[ \left( \frac{\rho}{r} \right)^{1/2} + \frac{1}{2} \left( \frac{\rho}{r} \right)^{3/2} \right]. \quad (26)$$

However, it was stated by Creager and Paris[15] that relations (20) and (21) have been derived for deep notches only. Because of the approximate nature of these equations, the stress concentration factor  $K_t$  given by relation (23) is lower than the accurate one. Therefore, the accuracy of eqns (25) and (26) will be improved if the accurate value of stress concentration factor  $K_t$ , determined independently of relation (23), is used.

In a notched body under bending load the nominal stress  $S$  varies linearly throughout the section ( $S_t \neq S$ )

$$S = S_t \left[ 1 - \frac{1}{x_0} \left( \frac{r}{\rho} - \frac{1}{2} \right) \right], \quad (27)$$

where  $x_0 = L/\rho$ . Therefore the variable nominal stress (27) should be included in eqns (25) and (26).

$$\sigma_x = \frac{K_t S_t}{2\sqrt{2}} \left[ \left( \frac{\rho}{r} \right)^{1/2} - \frac{1}{2} \left( \frac{\rho}{r} \right)^{3/2} \right] \left[ 1 - \frac{1}{x_0} \left( \frac{r}{\rho} - \frac{1}{2} \right) \right], \quad (28)$$

$$\sigma_y = \frac{K_t S_t}{2\sqrt{2}} \left[ \left( \frac{\rho}{r} \right)^{1/2} + \frac{1}{2} \left( \frac{\rho}{r} \right)^{3/2} \right] \left[ 1 - \frac{1}{x_0} \left( \frac{r}{\rho} - \frac{1}{2} \right) \right]. \quad (29)$$

It was found that if one uses the accurate value of the stress concentration factor  $K_t$ , a good stress estimation can also be obtained near relatively blunt notches. The comparison with the experimental data reported by Theocaris[16] and Theocaris and Marketos[17] is shown in Fig. 3. It is apparent that in the case of symmetrical semicircular notches, relation (26) gives

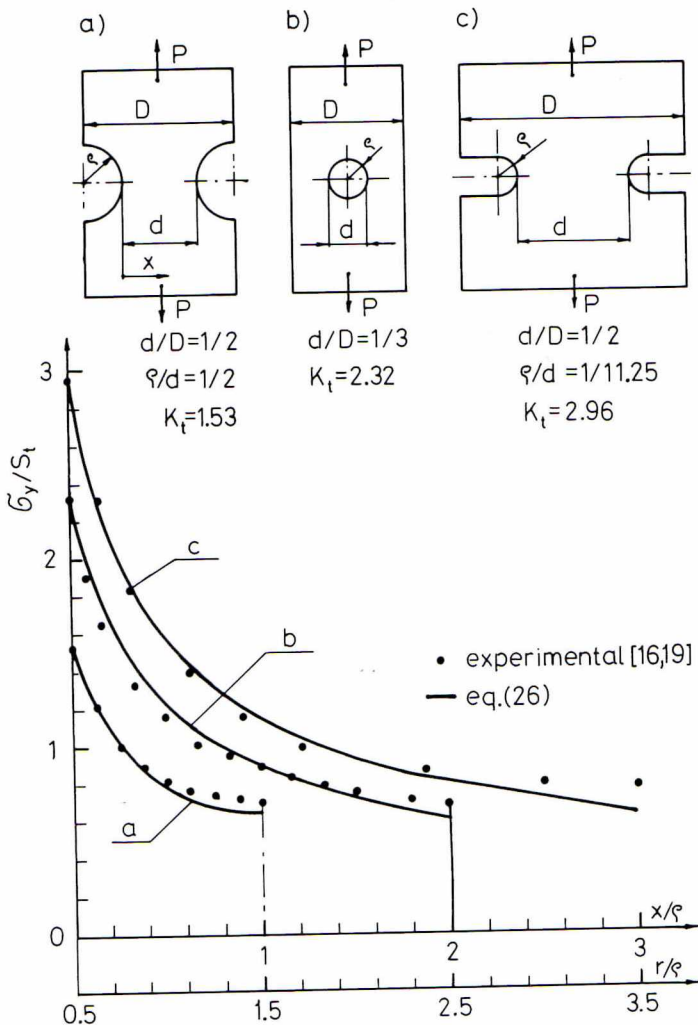


Fig. 3. Calculated and experimental elastic stress distribution near notches. (a) Specimen with two symmetrical semicircular notches. (b) Specimen with a central circular hole. (c) Specimen with two symmetrical U-notches.

good results over the entire net section. For symmetrical blunt U-notches, eqn (26) can be used over the distance  $3\rho$  from the crack tip with accuracy of  $\sim 7\%$ . In the case of the circular notch in the finite-width plate, shown in Fig. 3b, relation (26) was valid over almost the entire net section. For very blunt notches, such as the circular notch in an infinite plate or the semicircular notch in a semifinite plate, relation (26) gives a stress estimation with 10% accuracy over the distance  $1.5\rho$  from the notch tip.

Similarly, good notch-tip stress estimations can be obtained for bending on the basis of eqn (29). In the case of a bluntly notched compact tension specimen, shown in Fig. 4, a good agreement between eqn (29) and finite element calculations was achieved over the entire part of the tensile stress field.

Equations (25) and (26) or (28) and (29) represent some universal features of the elastic stress fields near notches. It can also be concluded that the stress field ahead of a notch tip can be satisfactorily defined by the stress concentration factor  $K_t$  and the notch tip radius  $\rho$ . A similar conclusion was also drawn by Schijve[18].

Because the equivalent energy density concept is based on the assumption of a localized plasticity, relations (25) and (26) or relations (28) and (29) are satisfactory for the approximate estimation of the notch-tip plastic zone size  $r_p$ .

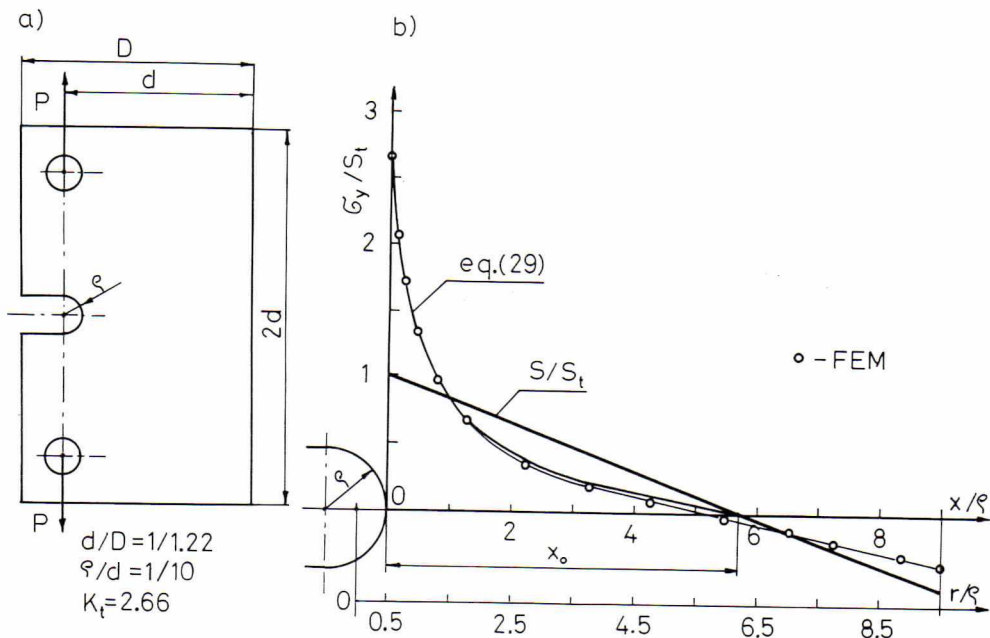


Fig. 4. The approximate and the FEM-calculated elastic stress distribution in a bluntly notched compact tension specimen. (a) Specimen shape and dimensions. (b) Elastic stress distributions.

#### *Estimation of the notch-tip plastic zone size*

The first approximation of the plastic zone size  $r_p$  ahead of a notch tip can be derived from the Hencky–Mises–Huber criterion on the basis of the elastic stress distribution discussed above. Under a plane stress state the plastic yielding criterion takes the form

$$\sigma_{ys} = \sqrt{(\sigma_x^2 - \sigma_x \sigma_y + \sigma_y^2)}. \quad (30)$$

Including eqns (25) and (26) into eqn (30) gives

$$\sigma_{ys} = \frac{K_t S_t}{2\sqrt{2}} \left[ \frac{\rho}{r_p} + \frac{3}{4} \left( \frac{\rho}{r_p} \right)^3 \right]^{1/2}. \quad (31)$$

An analogous relation can also be derived for a bending load by using eqns (28) and (29).

$$\sigma_{ys} = \frac{K_t S_t}{2\sqrt{2}} \left[ 1 - \frac{1}{x_0} \left( \frac{r_p}{\rho} - \frac{1}{2} \right) \right] \left[ \frac{\rho}{r} + \frac{3}{4} \left( \frac{\rho}{r} \right)^3 \right]^{1/2}. \quad (32)$$

Analytical calculation of the plastic zone size  $r_p$  from eqn (31) or eqn (32) is rather difficult, but it can easily be done numerically with the aid of a computer.

When the value of  $r_p$  is known the force  $F_1$  represented by the area  $F_1$  (Fig. 2) can be calculated by integrating eqns (26) or (29) for tension or bending, respectively:

a. for tension

$$\begin{aligned} F_1 &= \int_{\rho/2}^{r_p} \sigma_y \, dr - \sigma_y(r_p) \cdot (r_p - \frac{1}{2} \rho) \\ &= \frac{K_t S_t}{2\sqrt{2}} \rho \left[ 2 \left( \frac{r_p}{\rho} \right)^{1/2} - \left( \frac{\rho}{r_p} \right)^{1/2} \right] - \sigma_y(r_p) \cdot (r_p - \frac{1}{2} \rho), \end{aligned} \quad (33)$$

where

$$\sigma_y(r_p) = \frac{K_t S_t}{2\sqrt{2}} \left[ \left( \frac{\rho}{r_p} \right)^{1/2} + \frac{1}{2} \left( \frac{\rho}{r_p} \right)^{3/2} \right];$$

b. for bending,

$$\begin{aligned} F_1 &= \int_{\rho/2}^{r_p} \sigma_y \, dr = \sigma_y(r_p) \cdot (r_p - \frac{1}{2} \rho) \\ &= \frac{K_t S_t}{2\sqrt{2}} \rho \left[ \frac{2\sqrt{2}}{3x_0} - \frac{2}{3x_0} \left( \frac{r_p}{\rho} \right)^{3/2} + 2 \left( \frac{r_p}{\rho} \right)^{1/2} - \frac{2x_0 + 1}{2x_0} \left( \frac{\rho}{r_p} \right)^{1/2} \right] \\ &\quad - \sigma_y(r_p) (r_p - \frac{1}{2} \rho), \end{aligned} \quad (34)$$

where

$$\sigma_y(r_p) = \frac{K_t S_t}{2\sqrt{2}} \left[ 1 - \left( \frac{r_p}{\rho} - \frac{1}{2} \right) \frac{1}{x_0} \right] \left[ \left( \frac{\rho}{r_p} \right)^{1/2} + \frac{1}{2} \left( \frac{\rho}{r_p} \right)^{3/2} \right].$$

Due to the plastic yielding at the notch tip, the force  $F_1$  cannot be carried through by the material in the plastic zone  $r_p$ . But in order to satisfy the equilibrium conditions of the notched body, the force  $F_1$  has to be carried through by the material beyond the plastic zone  $r_p$ . As a result, stress redistribution occurs, increasing the plastic zone  $r_p$  by an increment  $\Delta r_p$  (Fig. 2).

If the plastic zone is small in comparison to the surrounding elastic stress field, the redistribution is not significant, and it can be interpreted as a shift of the elastic field over the distance  $\Delta r_p$  away from the notch tip. Therefore the force  $F_1$  is mainly carried through the material over the distance  $\Delta r_p$ , and therefore the force  $F_2$  (Fig. 2), represented by the area  $F_2$ , must be equal to  $F_1$ . Thus, the plastic zone increment  $\Delta r_p$  can be calculated from eqn (36).

$$F_1 = F_2 = \sigma_y(r_p) \cdot \Delta r_p. \quad (35)$$

Hence

$$\Delta r_p = F_1 / \sigma_y(r_p). \quad (36)$$

Substituting appropriate expressions for  $F_1$  and  $\sigma_y(r_p)$  we have:

a. for tension,

$$\Delta r_p = \rho \frac{[2(r_p/\rho)^{1/2} - (\rho/r_p)^{1/2}]}{[(\rho/r_p)^{1/2} + \frac{1}{2}(\rho/r_p)^{3/2}]} - \rho \left( \frac{r_p}{\rho} - \frac{1}{2} \right); \quad (37)$$

b. for bending,

$$\Delta r_p = \rho \frac{\left[ \frac{2\sqrt{2}}{3x_0} - \frac{2}{3x_0} \left( \frac{r_p}{\rho} \right)^{3/2} + 2 \left( \frac{r_p}{\rho} \right)^{1/2} - \frac{2x_0 + 1}{2x_0} \left( \frac{\rho}{r_p} \right)^{1/2} \right]}{\left[ \left( \frac{\rho}{r_p} \right)^{1/2} + \frac{1}{2} \left( \frac{\rho}{r_p} \right)^{3/2} \right] \left[ 1 - \left( \frac{r_p}{\rho} - \frac{1}{2} \right) \frac{1}{x_0} \right]} - \rho \left( \frac{r_p}{\rho} - \frac{1}{2} \right). \quad (38)$$

Finally, the correction factor for the energy density  $C_p$  at the notch tip (18a) can be written as follows:

a. for tension,

$$C_p = 1 + \left( \frac{\rho}{r_p} \right) \left\{ \frac{[2(r_p/\rho)^{1/2} - (\rho/r_p)^{1/2}]}{[(\rho/r_p)^{1/2} + \frac{1}{2}(\rho/r_p)^{3/2}]} - \left( \frac{r_p}{\rho} - \frac{1}{2} \right) \right\}; \quad (39)$$

b. for bending,

$$C_p = 1 + \left( \frac{\rho}{r_p} \right) \left\{ \frac{\left[ \frac{2\sqrt{2}}{3x_0} - \frac{2}{3x_0} \left( \frac{r_p}{\rho} \right)^{3/2} + 2 \left( \frac{r_p}{\rho} \right)^{1/2} - \frac{2x_0 + 1}{2x_0} \left( \frac{\rho}{r_p} \right)^{1/2} \right]}{\left[ \left( \frac{\rho}{r_p} \right)^{1/2} + \frac{1}{2} \left( \frac{\rho}{r_p} \right)^{3/2} \right] \left[ 1 - \left( \frac{r_p}{\rho} - \frac{1}{2} \right) \frac{1}{x_0} \right]} - \left( \frac{r_p}{\rho} - \frac{1}{2} \right) \right\}. \quad (40)$$

Because the correction factor  $C_p$  depends on the ratio  $(\rho/r_p)$ , it is satisfactory to solve eqn (31) or eqn (32) with respect to the ratio  $\rho/r_p$  only. Then the value of  $\rho/r_p$  can be used for calculating  $C_p$  from eqn (39) or eqn (40).

It should be noted that the plastic zone size  $r_p$  and the increment  $\Delta r_p$  were derived assuming constant stress  $\sigma_y(r_p)$  throughout the plastic zone. In fact, the stress  $\sigma_y$  in the plastic zone varies due to the strain hardening and the multiaxiality of the stress state. Therefore the correction factor  $C_p$  may slightly overestimate the effect of stress redistribution.

Knowing the value of  $C_p$ , we can solve the set of eqns (18) and (19) for any stress-strain curve. The numerical procedure described in reference [10] was used below.

### 3. COMPARISON OF CALCULATED AND EXPERIMENTAL DATA

#### *Monotonic loading*

Several different notches and materials were analyzed. For comparison the generalized Neuber rule[4, 10] was also used for calculation of the inelastic notch-tip stress and strain. The method was based on the following set of equations:

$$K_t^2 S_t e_t = \sigma_N e_N, \quad \epsilon_N = \frac{\sigma_N}{E} + \left( \frac{\sigma_N}{k} \right)^{1/n}, \quad e_t = \frac{S_t}{E} + \left( \frac{S_t}{k} \right)^{1/n}. \quad (41)$$

The results are presented in terms of plots of  $K_t S_t$  values against the calculated and measured strains in the notch tip. The results shown in Fig. 5 were obtained from symmetrical semicircular notches in a flat plate made of high-strength steel USST1. The stress concentration factor determined from reference [20] was  $K_t = 1.53$ . The material stress-strain curve, used for calculations, is also shown in Fig. 5. It can be concluded that the correction for plasticity  $C_p$  did not effect significantly the accuracy of notch-tip strain calculations, and both versions of the equivalent energy density can be used. The Neuber rule resulted in overestimation of the notch strains, as was similarly reported in references [6, 7]. The experimental results shown in Fig. 5 were reported by Theocaris[16].

Good results based on the energy method (Fig. 6) were also obtained for symmetrical edge notches[19] having flank angle 120°. The theoretical stress concentration factor determined

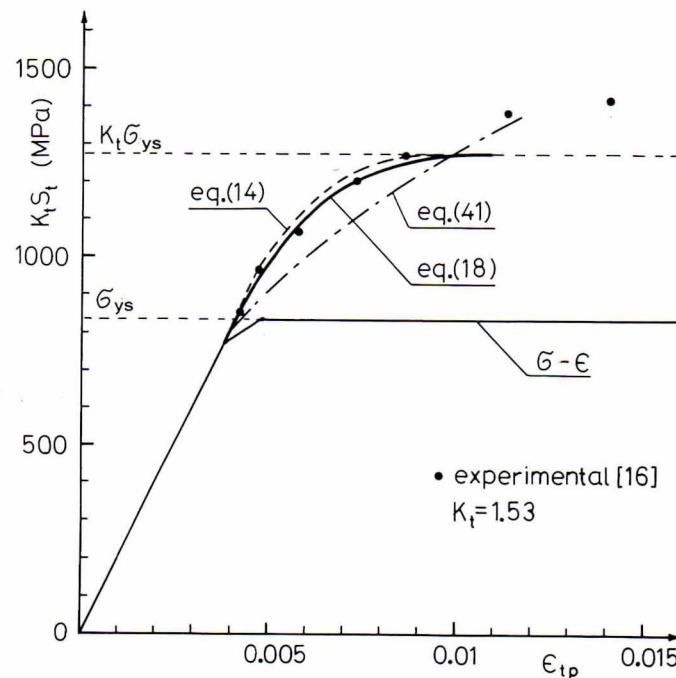


Fig. 5. Calculated and experimental notch strains in a specimen with two symmetrical semicircular edge notches (Fig. 3a, USS T1 steel[16]).

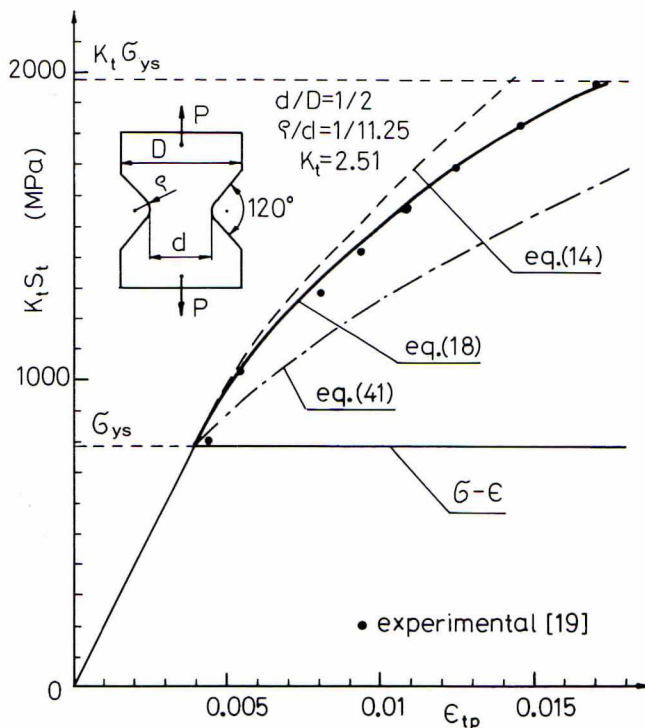


Fig. 6. Calculated and experimental notch strains in a specimen with two symmetrical V-notches (USS TI steel[19]).

from Neuber's diagrams[20] was  $K_t = 2.51$ . Specimens were made of high-strength steel, with stress-strain curve shown in Fig. 6. It is worth noting that in this case the correction for plasticity  $C_p$  apparently improves the accuracy of calculations, especially for high nominal stress  $S$ . The Neuber rule overpredicted again the notch-tip strains. It is also somewhat surprising that the energy concept gives good notch-tip strain prediction up to the general yielding, i.e. for  $S_t \leq \sigma_{ys}$ .

The inelastic strains in the tip of a central elliptical notch in a finite-width plate made of aluminium alloy 2024 T351 were measured by Leis *et al.*[21]. The comparison is shown in Fig. 7. It should be noted that the elliptical notch induced relatively high stress concentration  $K_t = 4.6$ , resulting in high inelastic strains. Again, better results were obtained when the plastic correction  $C_p$  was employed. Good results were obtained within the whole stress range  $0 \leq S_t \leq \sigma_{ys}$  (Fig. 7).

#### Constant amplitude cyclic loading

Notch-tip strains, due to a constant amplitude cyclic loading, measured in the keyhole SAE compact tension specimen made of high-strength steel RQC-100 were reported by Dowling *et al.*[13]. The calculations were based on the stabilized cyclic stress-strain curve in the form

$$\frac{\Delta \epsilon_{tp}}{2} = \frac{\Delta \sigma_{tp}}{2E} + \left( \frac{\Delta \sigma_{tp}}{2k'} \right)^{1/n'}. \quad (42)$$

Because the cyclic stress-strain curve correlates stress and strain ranges  $\Delta \sigma/2$  vs  $\Delta \epsilon/2$ , respectively, the nominal stress range  $\Delta S_t$  was also used for the energy density calculation. The same numerical procedure[10] as in the case of monotonic loading was applied. The experimental and calculated data are shown in Fig. 8 in the form of plots of the elastic notch-tip stress amplitude  $K_t \Delta S_t/2$  vs the inelastic notch-tip strain amplitude  $\Delta \epsilon_{tp}/2$ .

However, it was suggested by Dowling *et al.*[13] that, due to the relatively large thickness, a plane strain state would prevail in the notch tip. Therefore the "plane-strain" stress-strain curve  $\Delta \sigma_{tp}^b/2$  vs  $\Delta \epsilon_{tp}^b/2$  was used in calculations. The uniaxial "plane-stress"  $\Delta \sigma_{tp}/2$ -vs- $\Delta \epsilon_{tp}/2$

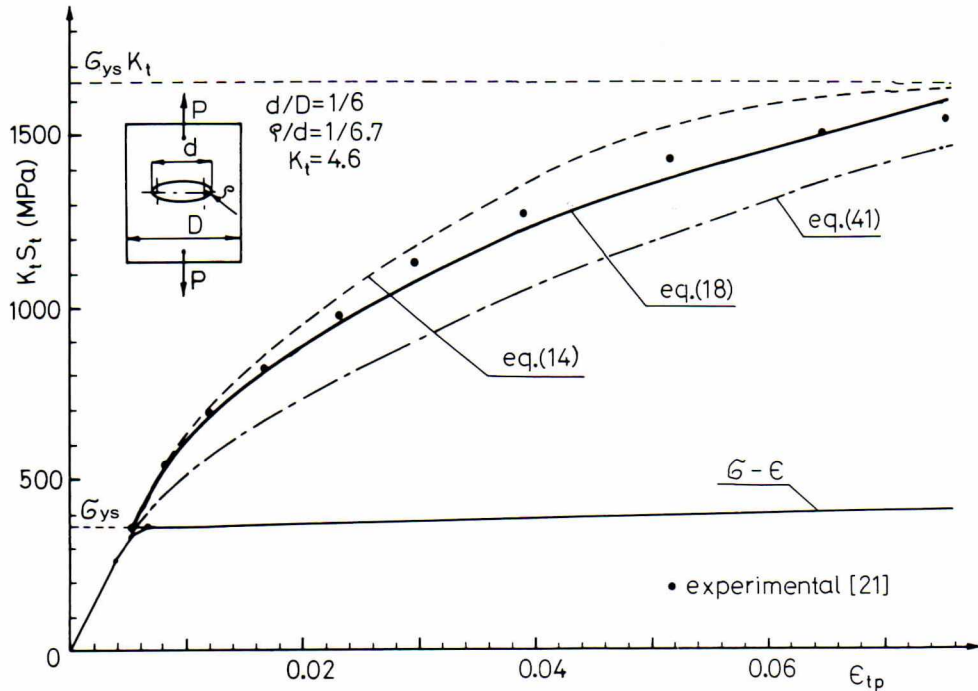


Fig. 7. Calculated and experimental notch strains in a specimen with a central elliptical notch, (Al 2024 T351[21]).

2 curve was translated into the biaxial “plane-strain”  $\Delta\sigma_{tp}^b/2$ -vs- $\Delta\epsilon_{tp}^b/2$  relation by using expressions (15) and (16). The “plane-stress” results calculated on the basis of the uniaxial stress-strain curve are also shown in Fig. 8. It is apparent that the “plane-strain” calculations, corrected for plasticity, were in the best agreement with the experimental data. Calculations based on the uniaxial stress-strain curve resulted in overestimation of the cyclic notch-tip strains.

It is worth noting that, due to the nominal stress gradient under bending load, the method can also be applied for a nominal notch-tip stress slightly higher than the yield strength, i.e.  $S_t > \sigma_{ys}$ . This is because the nominal stress  $S_t > \sigma_{ys}$  in bending may cause only localized plasticity, whereas under tension loading such stress causes plastic yielding of the whole section. Therefore, the stress energy density  $W_s$  due to the nominal stress  $S_t$  in bending should be calculated from relation (7) also for nominal notch-tip stress  $S_t > \sigma_{ys}$ .

#### Variable amplitude cyclic loading

Notch-tip strain history due to a variable amplitude cyclic loading was monitored by Moon *et al.*[6] at the tip of a central notch in a flat specimen made of aluminium alloy DTD-5014. The specimen and the stress-strain relations for the loading and unloading reversals, respectively, are shown in Fig. 9a. The nominal stress history and corresponding calculated and measured notch-tip strain histories are shown in Fig. 9b. The correction for plasticity  $C_p$  was used in calculations, assuming  $\sigma_{ys} = 411$  MPa and  $\sigma_{ys} = 660$  MPa for the loading and unloading reversals, respectively. Calculations based on the Neuber rule are also shown in Fig. 9b. The notch-tip strains were calculated subsequently for each reversal following the applied load history. The maximum stress  $\sigma_{tp \max}$  and maximum strain  $\epsilon_{tp \max}$  were calculated first by using the “loading” part ① of the stress-strain curve, then the notch-tip stress range  $\Delta\sigma_{tp}$  and strain range  $\Delta\epsilon_{tp}$  were calculated for the immediately following unloading reversal by using the “unloading” part ② of the stress-strain curve. The corresponding minimum stress  $\sigma_{tp \min}$  and minimum strain  $\epsilon_{tp \min}$  were calculated as

$$\sigma_{tp \min} = \sigma_{tp \max} - \Delta\sigma_{tp}, \quad \epsilon_{tp \min} = \epsilon_{tp \max} - \Delta\epsilon_{tp}. \quad (43)$$

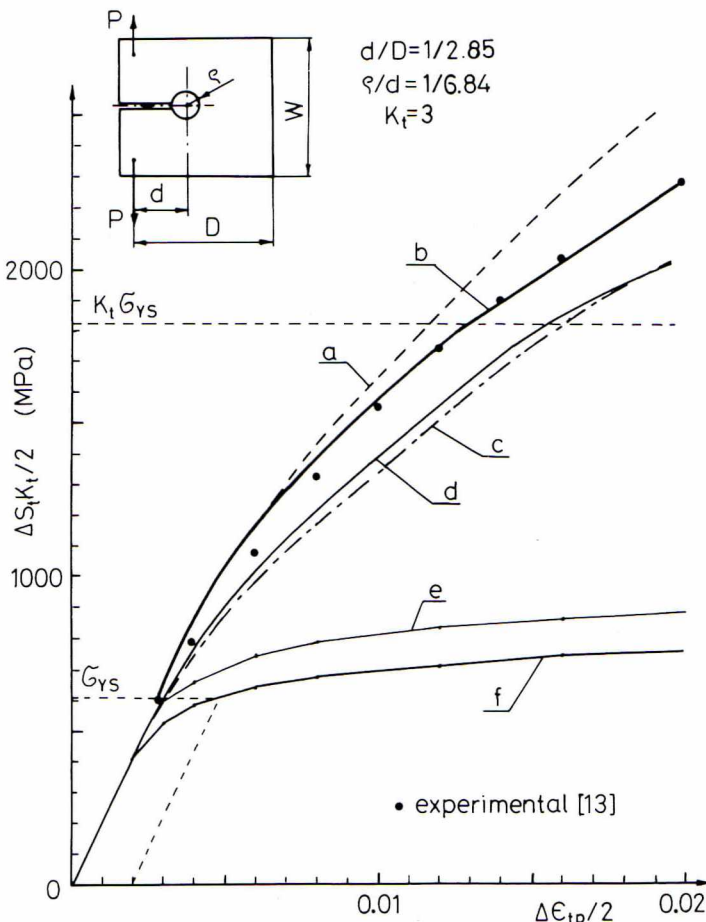


Fig. 8. Calculated and experimental notch strains in a keyhole SAE compact tension specimen under constant amplitude cyclic loading. (Steel RQC-100[13]): (a) plane strain —eqn (14); (b) plane strain—eqn (18); (c) plane strain—eqn (41); (d) plane stress—eqn (18); (e) plane strain  $\Delta\sigma^b - \Delta\epsilon^b$  curve; (f) plane stress  $\Delta\sigma - \Delta\epsilon$  curve.

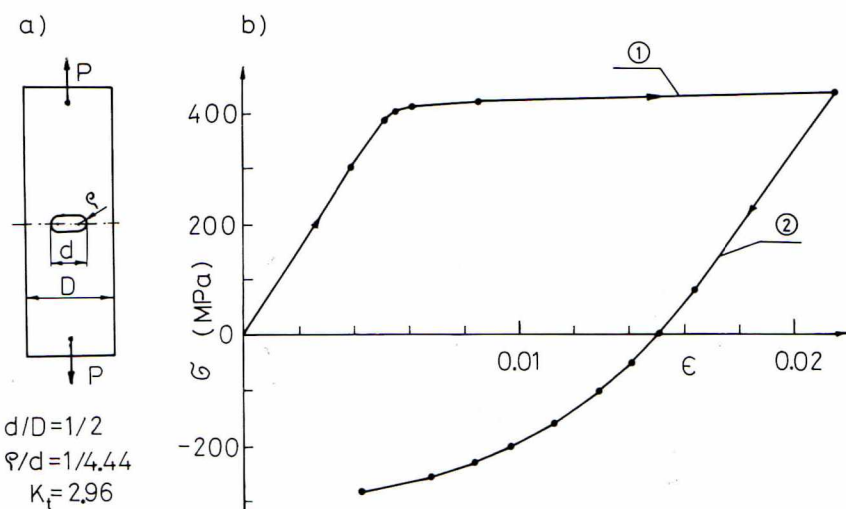


Fig. 9a. Specimen with a central notch and the stress-strain relation for the aluminium alloy DTD-5014[6]. (a) Specimen geometry and dimensions. (b) Stress-strain behaviour; ①—loading reversals, ②—unloading reversals.

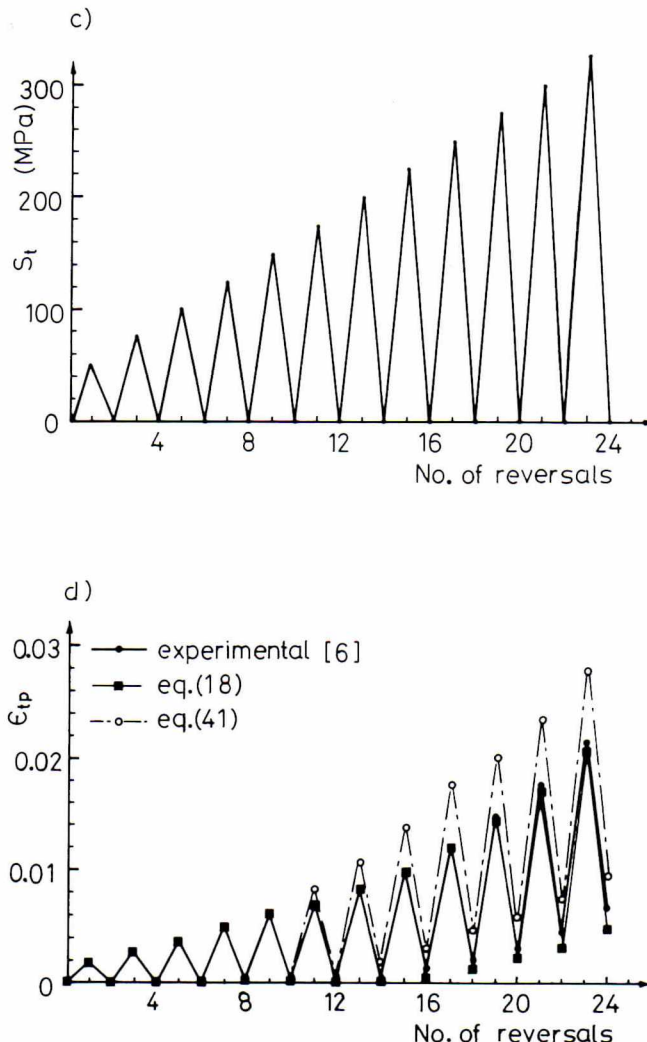


Fig. 9b. Applied nominal stress history  $S_t$  and corresponding calculated and experimental notch-tip strain histories (DTD-5014[6]). (c) Nominal stress history  $S_t$  in the notch tip. (d) Calculated and measured notch-tip strain histories.

The calculated maximum and minimum strain values made it possible to determine the whole notch-tip strain history shown in Fig. 9b.

The agreement between the measured and calculated strain histories was good throughout the entire load history. However, it should be noted that in the case of cyclic loading the stress-strain relation changes from reversal to reversal. Therefore, a material model simulating the stress-strain behaviour under cyclic loading has to be applied together with the equivalent energy concept. The simple procedure described above was possible because of the simple ascending load pattern. In the case of a more irregular load history, a special cyclic counting procedure and material stress-strain model[1, 23] has to be employed.

Good results were also obtained for bluntly notched compact tension specimens shown in Fig. 4. The inelastic notch-tip strains were determined by Karlsson[22], using the finite element method. The reversal-by-reversal procedure was applied for the strain history calculation using the stress-strain curves shown in Fig. 10. The “unloading” part of the stress-strain curve ② was obtained by expansion[1] of the basic cyclic stress-strain curve ① by a factor of 2. The nominal stress history  $S_t$  and the corresponding calculated notch-tip strain history are also shown in Fig. 10. Regardless of the advanced plasticity ahead of the notch tip, the calculated strain history was very close to that determined by the finite element method.

Neuber's rule overpredicted the notch-tip strains also under cyclic loads.

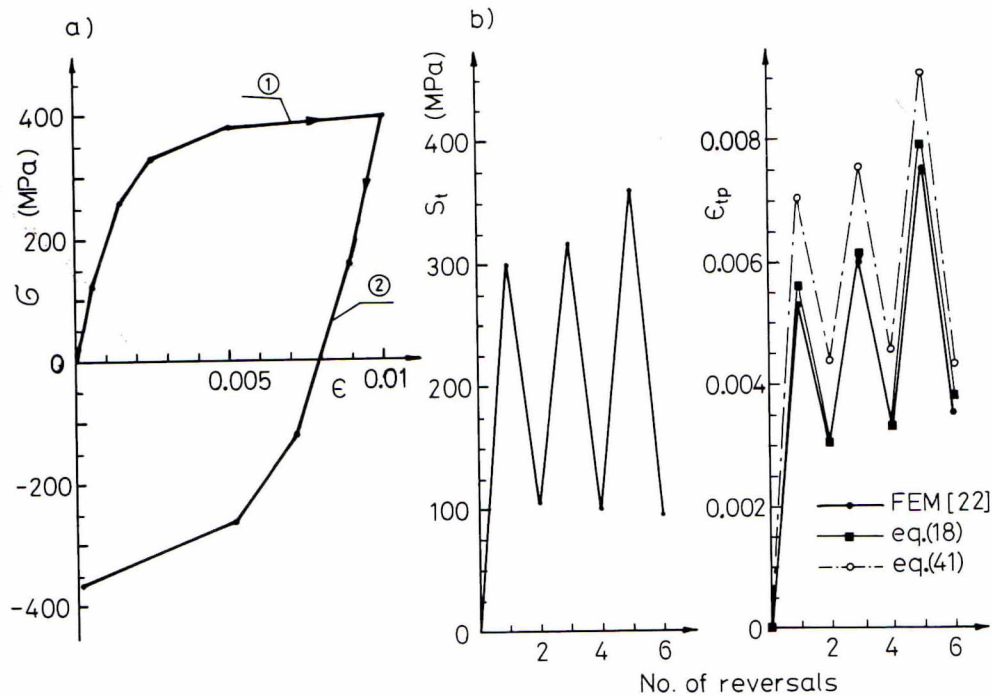


Fig. 10. FEM-calculated[22] and the energy based notch-tip strain histories in a bluntly notched compact tension specimen shown in Fig. 4. (a) Cyclic stress-strain behaviour; ①—loading reversals, ②—unloading reversals. (b) Applied nominal notch-tip stress  $S_t$  history. (c) Calculated notch-tip strain histories.

#### 4. CONCLUSIONS

It was found that the energy density method gave good results for low and high stress concentration factors. The method can be used within the nominal stress range  $0 \leq S_t \leq \sigma_{ys}$ . However, under the high nominal stress  $S_t$ , approaching the yield strength  $\sigma_{ys}$ , correction for the plastic stress redistribution should be applied. The correction for plasticity  $C_p$  is especially important for notches with high stress concentration factors  $K_t > 2$  and for high nominal stresses  $0.8 \sigma_{ys} \leq S_t \leq \sigma_{ys}$ . The equivalent energy density method can be used for both monotonic and cyclic loadings. However, in the case of cyclic loading, a material model for stress-strain behaviour under cyclic loading must be employed together with the equivalent energy method. The method can be applied to both tensile and bending loads. It is also worth noting that under bending loads the method gave good notch-tip strain estimation for nominal notch-tip stresses above the yield strength, i.e. for  $S_t > \sigma_{ys}$ . It was possible because under bending load the theoretical nominal notch-tip stress  $S_t > \sigma_{ys}$  does not necessarily cause general yielding of the whole section. Therefore, by assuming  $K_t = 1$  the local elastic-plastic strains and stresses in a smooth specimen under bending can also be calculated.

It was shown that the elastic stress field in the neighbourhood of the notch tip can be satisfactorily characterized in a general form by the notch tip radius  $\rho$ , the stress concentration factor  $K_t$  and the gradient of the nominal stress  $S$ .

In most cases the disagreement between the measured and calculated strains was below 10%, regardless of the material stress-strain curve, stress concentration factor and notch geometry.

The equivalent strain energy density method is suitable for numerical calculations and all kinds of stress-strain relations. However, this method was verified for tensile and bending loads only. It has not yet been verified for torsional loading.

#### REFERENCES

- [1] Fatigue under complex loading. In *Advances in Engineering*, vol. 6 (Edited by R. M. Wetzel), Society of Automotive Engineers, SAE Warrendale, Pa. (1979).

- [2] T. Seeger, A. Beste and A. Amsutz, Elastic-plastic stress-strain behaviour of monotonic and cyclic loaded notched plates. *Fracture 1977, Proc. 4th Int. Conf. on Fracture ICF4* (Edited by D. M. R. Taplin), pp. 943-951. University of Waterloo Press, Ontario (1977).
- [3] H. Neuber, Theory of stress concentration for shear-strained prismatic bodies with arbitrary nonlinear stress-strain law. *J. Appl. Mech.* **28**, 544-551 (1961).
- [4] T. Seeger and P. Heuler, Generalized application of Neuber's rule. *J. Test. Eval.* **8**, 199-204 (1980).
- [5] T. H. Topper, R. M. Wetzel and JoDean Morrow, Neuber's rule applied to fatigue of notched specimens. *J. Mater. (JMLSA)* **4**, 200-209 (1969).
- [6] J. E. Moon, B. H. E. Perret and P. R. Edwards., *A Study of Local Stress Histories in Loaded and Unloaded Holes and their Implications to Fatigue Life Estimation*. Aeronautical Research Council, Paper C.P. No. 1374, London (1977).
- [7] G. Glinka, *Fatigue Crack Initiation and Propagation*. Scientific Report No. 75, Mechanics, Warsaw Technical University, Warsaw (1981) (in Polish).
- [8] A. Conle and H. Nowack, Verification of a Neuber-based notch analysis by the companion specimen method. *Experimental Mech.* **17**, 57-63 (1977).
- [9] K. Molski and G. Glinka, A method of elastic-plastic stress and strain calculation at a notch root. *Mat. Sci. Engng* **50**, 93-100 (1981).
- [10] G. Glinka, Energy density approach to calculation of inelastic strain-stress near notches and cracks. *Engng Fracture Mech.* **22**, 485-508 (1985).
- [11] J. W. Hutchinson, Singular behaviour at the end of a tensile crack in a hardening material. *J. Mech. Phys. Solids* **16**, 13-31 (1968).
- [12] J. Polak, Stress and strain concentration factor evaluation using the equivalent energy concept. *Mat. Sci. Engng* **61**, 195-200 (1983).
- [13] N. E. Dowling, W. R. Brose and W. K. Wilson, Notched member fatigue life predictions by the local strain approach. In *Advances in Engineering*, vol. 6 (Edited by R. M. Wetzel), pp. 55-84. Society of Automotive Engineers, SAE Warrendale, Pa. (1979).
- [14] G. R. Irwin, Linear fracture mechanics, fracture transition and fracture control. *Engng Fracture Mech.* **1**, 241-257 (1968).
- [15] M. Creager and P. C. Paris, Elastic field equations for blunt cracks with reference to stress corrosion cracking. *Int. J. Fracture Mech.* **3**, 247-252 (1967).
- [16] P. S. Theocaris, Experimental solution of elastic-plastic plane-stress problems. *J. Appl. Mech.* **29**, 735-743 (1962).
- [17] P. S. Theocaris and E. Marketos, Elastic-plastic analysis of perforated thin strips of a strain-hardening material. *J. Mech. Phys. Solids* **12**, 377-390 (1964).
- [18] J. Schijve, Stress gradients around notches. *Fatigue Engng Mat. Struct.* **5**, 325-332 (1982).
- [19] P. S. Theocaris and E. Marketos, Elastic-plastic strain and stress distribution in notched plates under plane stress. *J. Mech. Phys. Solids* **11**, 411-428 (1963).
- [20] M. Neuber, *Kerbspannungslehre*. Springer-Verlag, Berlin and Heidelberg (1958).
- [21] B. N. Leis, C. Govda and T. Topper, Some studies of the influence of localized and gross plasticity on the monotonic and cyclic concentration factors. *J. Test. Eval.* **1**, 341-348 (1973).
- [22] A. Karlsson, Crack initiation at notches. *Proc. 3rd Int. Conf. Numerical Methods in Fracture Mechanics* (Edited by A. Luxmoore and R. Owen), pp. 619-630. Pineridge Press, Swansea, U.K. (1984).
- [23] Z. Mroz, Hardening and degradation rules for metals under monotonic and cyclic loading. *J. Engng Mat. Tech.* **105**, 113-121 (1983).

(Received 4 December 1984)